



CORROSION STUDY OF A CARBON STEEL IMMERSSED IN CONCRETE ALTERNATIVE BY ELECTROCHEMICAL FREQUENCY MODULATION

W. APERADOR^{a,*}, E. RUIZ^a and J. BAUTISTA-RUIZ^b

^aSchool of Engineering, Universidad Militar Nueva Granada, BOGOTÁ, COLOMBIA

^bUniversidad Francisco de Paula Santander, San José de Cúcuta, COLOMBIA

ABSTRACT

The electrochemical frequency modulation technique is an electrochemical technique used to determine the corrosion rate in steel embedded in concrete made with mixtures of fly ash and steel slag alkali activated and exposed to accelerated carbonation. This technique uses two signals input AC voltage; and has the quality of each signal has a different frequency, these signals are applied to reinforced concrete. As the current is a nonlinear function of the potential, the system responds in a nonlinear manner to the excitation potential is obtained as a measurement of response current in this response sum components they are jointly involved difference and multiples of the input frequency. This technique uses causality factors, which can verify experimental data, finds the exact values of the corrosion current density, the corrosion current and obtaining the cathodic and anodic slopes. The characterization of cementitious materials, was performed by X-ray diffraction. It was determined that mixtures containing steel slag generate low corrosion rate values.

Key words: Modulation frequency, Corrosion, Steel slag, Fly ash.

INTRODUCTION

Techniques for evaluating the corrosion phenomena are widely used because of the ease of making measurements in almost any system regarding these techniques, have the non-destructive techniques such as linear polarization resistance (LPR) one of the most important disadvantages of the LPR technique is that by itself delivers an approximate value of polarization resistance¹⁻³, since the system remains in "quasi-equilibrium" states thermodynamic due to small voltages that apply ± 20 mV; and deliver a value of corrosion rate is necessary to assume or tab-known both anode and cathode slopes process^{4,5}. In order to meet these outstanding and they could be tabulated; in many cases the technique Tafel

* Author for correspondence; E-mail: g.ing.materiales@gmail.com

polarization curves where the quasi-thermodynamic equilibrium is removed^{6,7}, the material is passive and then oxidized thus leading to the destruction of the material and sacrificing a sample to obtain required values on the LPR technique^{8,9}, another widely used technique is the Electrochemical impedance spectroscopy (EIS), the problem with this technique is that other parameters must be known in order to give a value of speed of deterioration of materials evaluated; but other destructive technique widely used is the Tafel polarization technique is destructive because it applies a high potential above the equilibrium potential, generating oxidation processes on the test material¹⁰⁻¹⁴.

The technique electrochemical frequency modulation (EFM): It was proposed by Bogaerts, as an alternative method for monitoring the corrosion rate in different conductive materials. It consists of two sinusoidal potential signal summed and applied to a sample to be evaluated against corrosion by means of a potentiostat. The potential amplitude perturbation is 10-20 mV, and disturbance frequencies of each of the signals are 2 Hz and 5 Hz¹⁵⁻¹⁹.

The development and application of cementitious materials by alkaline activation of aluminosilicate such as blast furnace slag and fly ash is gaining importance, for the need for developing sustainable construction materials²⁰⁻²². Alkali-activated cements also called geopolymers can be synthesized by mixing an alkaline solution with a source of aluminosilicates such as fly ash or blast furnace slag. These have proven to be a valuable alternative for use in concrete production²³. Among the alkali activated cementitious systems, fly ash and granulated blast furnace slag have been the most studied materials. This is due to the optimum activation process presented, and the formation of cementitious products generated in the slag by the gel C-(A)-S-H and ashes by gel formation the gel N-A-S-H and zeolites as side reaction products²⁴.

The performance of the mixtures of fly ash and alkali activated slag it depends primarily on the chemical composition of alkali precursors, the nature and quality of pozzolanic materials and methods of curing of concrete²². The concentration of the alkaline activator is one of the key variables in the process of geopolymerization; since the solubility of the aluminosilicate is increased with increasing hydroxide ion concentration²⁵. Based on the foregoing, it is significant that although there are many related alkaline activation of aluminosilicate material works; a clear design methodology has not been demonstrated²¹.

In this paper, nonlinear electrochemical technique for monitoring corrosion rate was implemented by intermodulation distortion (IMD), also known as electrochemical frequency modulation (EFM). With this technique, the corrosion rate can be obtained instantly, without previous knowledge of the Tafel parameters (pending cathodic and

anodic). It was determined that pozzolanic materials mixtures containing fly ash show a lower performance durability.

EXPERIMENTAL

Mixtures were made they used as cementitious: granulated blast furnace slag and fly ash activated with sodium silicate (Na_2SiO_3) at a concentration of 5% Na_2O , expressed as weight percent slag or ash to incorporate. The manufacture of concrete mixtures in both cases containing a dosage of cementitious material 320 kg/m^3 . It is assumed that the water/cement and water activating solution +/+ ash slag is equivalent in both cases this ratio was 0.5 in order to obtain a corresponding seating provides of 89 mm.

The type, composition, size of fine and coarse aggregate was the same for the mixtures obtained. Correspond to a gravel maximum size of 21 mm, specific gravity of 3.05 g/cm^3 , compact unit mass of 1.69 kg/cm^3 , unit mass release of 1.84 kg/cm^3 , and absorption of 1.3%. A sand surface area of 2.54 g/cm^3 , compact unit mass of 1.38 kg/cm^3 , loose unit weight of 1.64 kg/cm^3 , absorption of 3.2%. Curing of the mixtures was performed using a controlled curing approximately 90% relative humidity and a constant temperature environment of 20°C . Subsequently, the samples were subjected to the entry of CO_2 by a camera which enables to control the temperature, humidity and CO_2 , with 3% carbon dioxide, 25°C and 90% relative humidity, this was done through full carbonation of concrete.

It was used commercial structural steel reference ASTM A706 commonly used in earthquake-resistant constructions with a diameter of 1/8" and without pretreatment. In the corrosion tests, this acted as a working electrode. For the development of electrochemical tests, it was used as the external reference electrode copper-copper sulfate analytic. A graphite electrode immersed in the test tubes served as counter electrode in all the tests.

Electrochemical measurements were conducted during the carbonation process in a time interval of nine months. To determine the degree of corrosion of steel rods, the electrochemical technique of frequency modulation using an electrochemical potentiostat-galvanostat was used.

The characterization of the raw material was performed by X-ray diffraction (XRD), using a PW3050/60 (θ/θ) goniometer, managed under a system XPERT-PRO using a Cu Ka monochromatic radiation of 1.54 \AA , operated at 40 kV and 40 mA under the temperature conditions of 25°C . The sweep on the surface was made from $2\theta = 20.01^\circ$ to $2\theta = 99.99^\circ$ with $2\theta = 0.02^\circ$ step time of 0.1 seconds sweep. The crystalline phases of the steel surface was observed with an X-ray diffractometer, XPERT-PRO, using the database diffraction

equipment, also the MAUD program, which analyzes by the Rietveld method, which is used to adjust a theoretical diagram to coincide entirely with the observed. Such theoretical patterns are obtained based on the crystal structures and parameters. The process of identification of compounds was performed before making its alkaline activation.

RESULTS AND DISCUSSION

Characterization of raw materials

In Fig. 1, the spectrum of X-ray diffraction, of granulated steel slag is observed. The phase identification was carried out from interatomic distribution densities. In the spectrum it is determined that the slag is composed by a large percentage tridymite, also known as silicon oxide (SiO_2) stabilized with an alkali metal^{26,27}; corresponds to an inorganic mineral with a monoclinic crystal system with the following parameters: $a = (\text{Å})$: 18.4940, $b = (\text{Å})$: 4.9910, $c = (\text{Å})$: 23.7580 Alpha ($^\circ$): Beta = 90.0000 ($^\circ$): 105.7900 and Gamma ($^\circ$) = 90.0000; with a number of PDF - 18-1170 (PDF: Powder Difraccion File). The Tridymite is obtained due to process synthesized because there is no natural way for training, because it requires a synthesis temperature of 1100°C. The other compound corresponds to Mayenite; which is mixed with calcium oxide crystals-aluminum oxide (12/7), the chemical formula $\text{Al}_{14}\text{Ca}_{12}\text{O}_{33}$ (PDF-), has a cubic crystal system with the following parameters: $a = (\text{Å})$: 11.9890 $b = (\text{Å})$: 11.9890 $c = (\text{Å})$: 11.9890; Alpha ($^\circ$): 90 Beta ($^\circ$): 90 Gamma ($^\circ$): 90; mayenite type compound is a system in which a part or all of free oxygen ions in the lattice are replaced by other anions within the range in which are kept in a lattice of Ca and a cell structure formed by AlO type compound, oxygen in the cell is replaced by electrons through treatment and form a composite of mayenite conductive²⁸. Another mineral with a small percentage in the mezcla it is Srebrodolskite a PDF-01-074-0802,²⁹ its chemical formula is $\text{Ca}_2\text{Fe}_2\text{O}_5$ corresponds to a type orthorhombic crystal system with the following parameters: $a = (\text{Å})$: 5.3900 $b = (\text{Å})$: 14.6800 $c = (\text{Å})$: 5.6400 Alpha = Beta = Gamma = ($^\circ$): 90. The Srebrodolskite is a stable compound formation due to high temperatures.

Another similar to above that is present in the mixture is Diiron (III) Dialuminium Tetracalcium Oxide also known as brown millerite (PDF compound - 01-074-0803), which has the following components $\text{Al}_2\text{Ca}_4\text{Fe}_2\text{O}_{10}$ also has an orthorhombic structure, with the following parameters $a = (\text{Å})$: 5.3400 $b = (\text{Å})$: 5.5800 $c = (\text{Å})$: 14.5000; Alpha ($^\circ$): 90 Beta ($^\circ$): 90 Gamma ($^\circ$): 90³⁰; this material is one of the responsible of the hydraulic properties, which has the slag additionally this compound is also found in traditional Portland cements, the brownmillerite is stable at a temperature of 1200°C. Therefore, the product has a similar transformation to a clinker composition³¹. The dialuminium magnesium oxide (PDF-01-073-2210), is a compound that has been identified as a major minerals steel furnace slag is

mainly due to the magnesium content in the slag used in this study, has one cubic structure, with the following parameters $a = (\text{\AA})$ $b = 8.0800 (\text{\AA})$ $c = 8.0800 (\text{\AA})$: 8.0800.

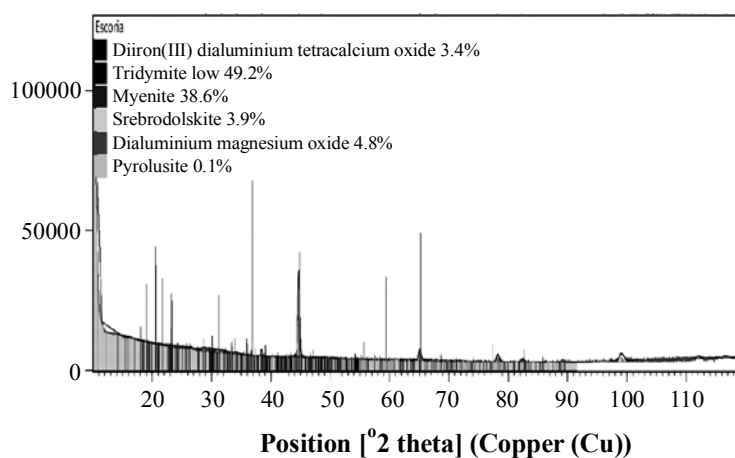


Fig. 1: Diffraction pattern of the steel blast furnace slag X-rays, determining the phases present in the cementitious mixture

In Fig. 2, the spectrum of X-ray diffraction of the fly ash (FA) this type has a structure aluminosilicate gel (geopolymer), composed mainly of calcium magnesium carbonate (Dolomite) shows PDF-36-426³² known as limestone, which has a chemical formula corresponding to $C_2Ca_1Mg_1O_6$, has a hexagonal crystal structure with the following parameters $a = (\text{\AA})$: 4.8030; $b = (\text{\AA})$ and $c = 4.8030 (\text{\AA})$: 15.9840, dolomite is consisting essentially of alkaline features providing hydrated aluminosilicates, magnesium oxides present in the system stable form silicates of magnesium, responsible for the mechanical properties of the solid material. The other compound is Aluminium Silicon Oxide (PDF-01-074-4146), called mullite with the following chemical formula $Al_{4.68} O_{9.66} Si_{1.32}$, has an orthorhombic crystal structure with the following parameters $a = (\text{\AA})$: 7.5760 ; $b = (\text{\AA})$ and $c = 7.6910 (\text{\AA})$: 2.8880, This compound is formed because the silica is in equilibrium with alumina or oxides of calcium or iron, leading to the crystallization of mullite, corresponding to a aluminosilicatada glassy phase, therefore this material is of particular interest to obtain cementitious materials. The other compound is the Quartz (PDF - 98-010-7202) is the minority inorganic phase present in the fly ash.

Determination of corrosion rates

For analysis of the EFM technique input frequencies of 2 Hz and 5 Hz was used; with amplitudes of 20 mV over 4 cycles, simultaneously applied to the electrochemical cell by potentiostatic system. EFM technique; in contrast to LPR and EIS techniques, it has the

advantage that the corrosion rate calculated without prior knowledge of Tafel slopes. Moreover, the EFM measure also gives a self-check in the internal shape of the two causal factors. These two factors should have the values 2.0 and 3.0 if all conditions of the theory of EFM are resolved correctly³³.

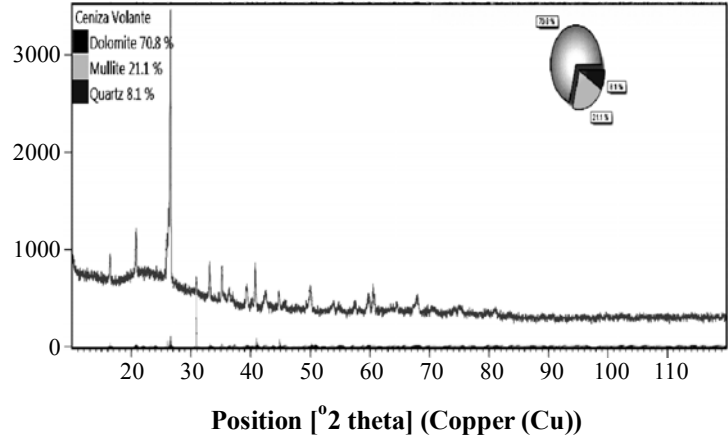


Fig. 2: Diffraction pattern of X-rays fly ash where dolomite, mullite and quartz phases is determined present in the cementitious material

The frequency spectrum obtained from the response current (Figs. 3 and 4) contains harmonic components and intermodulation frequencies. Between these components there is some relationship, which it is given by:

$$i_{\omega_2 \pm \omega_1} = 2i_{2\omega_1} = 2i_{2\omega_2} \quad \dots(1)$$

$$i_{2\omega_2 \pm \omega_1} = i_{2\omega_1 \pm \omega_2} = 3i_{3\omega_1} = 3i_{3\omega_2} \quad \dots(2)$$

This relationship is the basis for determining causality factors, which are given as follows:

$$\text{Causality Factor (2): } \frac{i_{\omega_2 \pm \omega_1}}{i_{2\omega_1}} \quad \dots(3)$$

$$\text{Causality Factor (3): } \frac{i_{2\omega_2 \pm \omega_1}}{i_{3\omega_1}} \quad \dots(4)$$

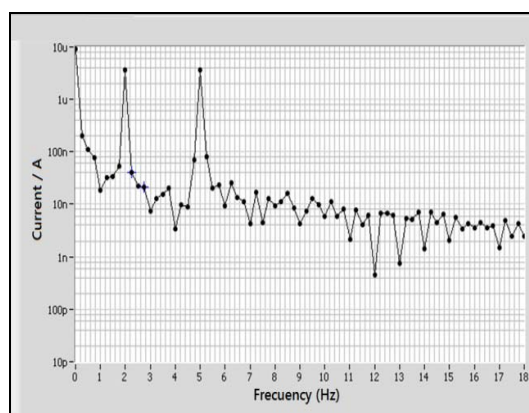
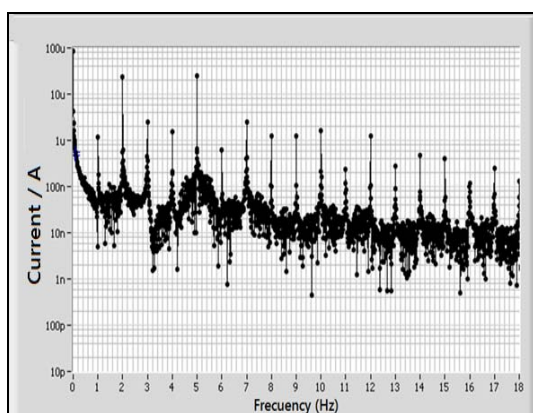
The causality factors are used to validate the data, they are calculated of the frequency spectrum of the response current. If these factors differ significantly from the

theoretical values, 2 and 3, it can be concluded that the measures are influenced by noise. If the causality factors are approximately equal to the predicted values of 2 and 3 there is a causal relationship between the disturbance signal and the feedback signal. Then it is assumed that the data are reliable.

The equations set forth above are based on a Taylor series. The terms of the Taylor series with an order greater than 3 they are unnecessary because current magnitude of these terms is easily confused with the noise generated during the test. However, the equations are valid only when the signal amplitude potential is sufficiently small (the amplitude should not exceed the region of low distortion). More precisely, the relationship between the amplitude and the Tafel parameter perturbation shown to be much less than 1.

$$\frac{U_0}{\beta_a} \ll 1, \frac{U_0}{\beta_c} \ll 1 \quad \dots(5)$$

The measures found in concrete made from fly ash (FA) (Fig. 3) shows that the corrosion potential has a tendency to diminish their value in each of the assessed levels, since this parameter decreases considerably when the concrete is subjected to accelerated carbonation³⁴. The corrosion potential of specific FA moves more negative potentials, as analyzed in time, showing potential corresponding assets of 6 to 9 months evaluation. Regarding corrosion currents shown in Table 1, this value increases about three times in the three-month evaluation compared evaluation start time (28 days curing), for the six months it is that this value is quadrupled compared to found in the initial value. Since the corrosion rate is directly proportional to the corrosion current, these values increase as the assessment is made in time, finding values 2 times higher compared to the initial evaluation. At 9 months carbonation values are 10 times that found for the start of the evaluation.



Cont...

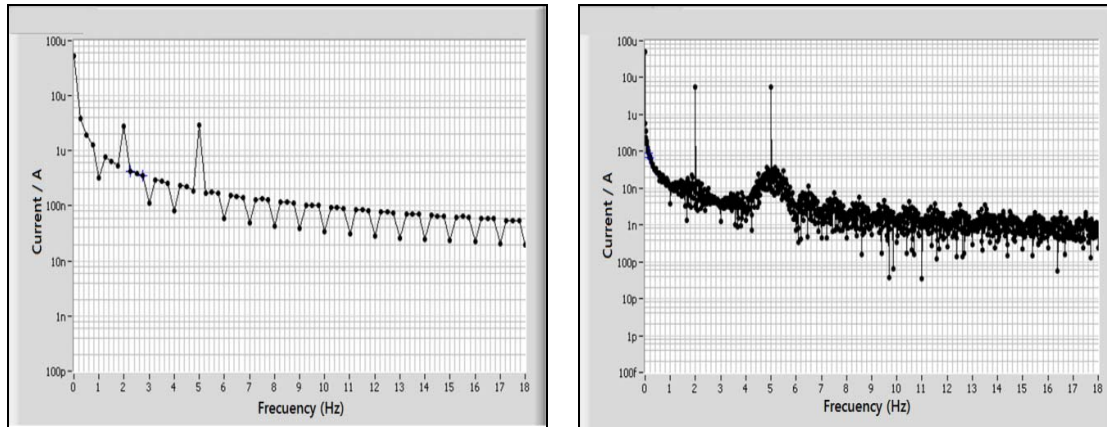


Fig. 3: EFM spectra, found in each of the levels of the samples of fly ash (a) 0 hrs; (b) 3-month assessment; (c) 6-month evaluation; (d) 9 months evaluation

In Table 1, it can be seen that the corrosion potential obtained with this technique indicates that are obtained more negative potentials according as assessment progresses. Regarding the corrosion currents and corrosion rate, we can see that this material is affected by the entry of carbon dioxide, because the corrosion current is increased, indicating a logarithmic increase corrosion density, this increase creates a proportional increase in the corrosion rate, as a result was obtained that the material has an involvement in its entirety generating corrosive processes are accelerated as the CO_2 penetrates the material for this reason is more affected its layer protective.

Table 1: Parameters supplied with the EFM technique for concrete obtained from fly ash

	E_{corr} (mV vs Cu/CuSO ₄)	I_{corr} ($\mu\text{A}/\text{cm}^2$)	V_{corr} (mpy)	Causality Factors 2	Causality Factors 3
0 hrs	-289	10.3	0.34	2.3	3.2
3 months	-635	31.7	2.25	2.1	3.0
6 months	-652	43.5	2.49	2.3	3.2
9 months	-629	78.3	3.22	1.8	3.1

In Fig. 4, the response of the application of the EFM technique for concrete obtained from the steel slag (GBFS) is obtained here shows that the variation of the current for each of the cases studied ranges from μA to the ηA because of this they are low corrosion current value, thus indicating low corrosion rate values.

GBFS concrete just like concrete FA found subjected to accelerated CO₂ system, carbonation of concrete GBFS is somewhat slower, because of this, lower corrosion rate parameters are obtained. In Fig. 4a, the concrete is evaluated at 0 hrs, resulting in an overall anodic dissolution, followed by the formation of a passive region³⁵. To the specimen evaluated at 3 months passivation zone observed, regarding the corrosion current, it is obtained that the concrete has generated a more compact passivating layer so corrosion density has decreased, when observing the concrete 6 months general dissolution and the area of passivation is determined has it decreased as the corrosion potential is observed more negative, causing a more active material, the density of corrosion of this material significantly increases with respect to three months, this same behaviour seen until 9 months of evaluation.

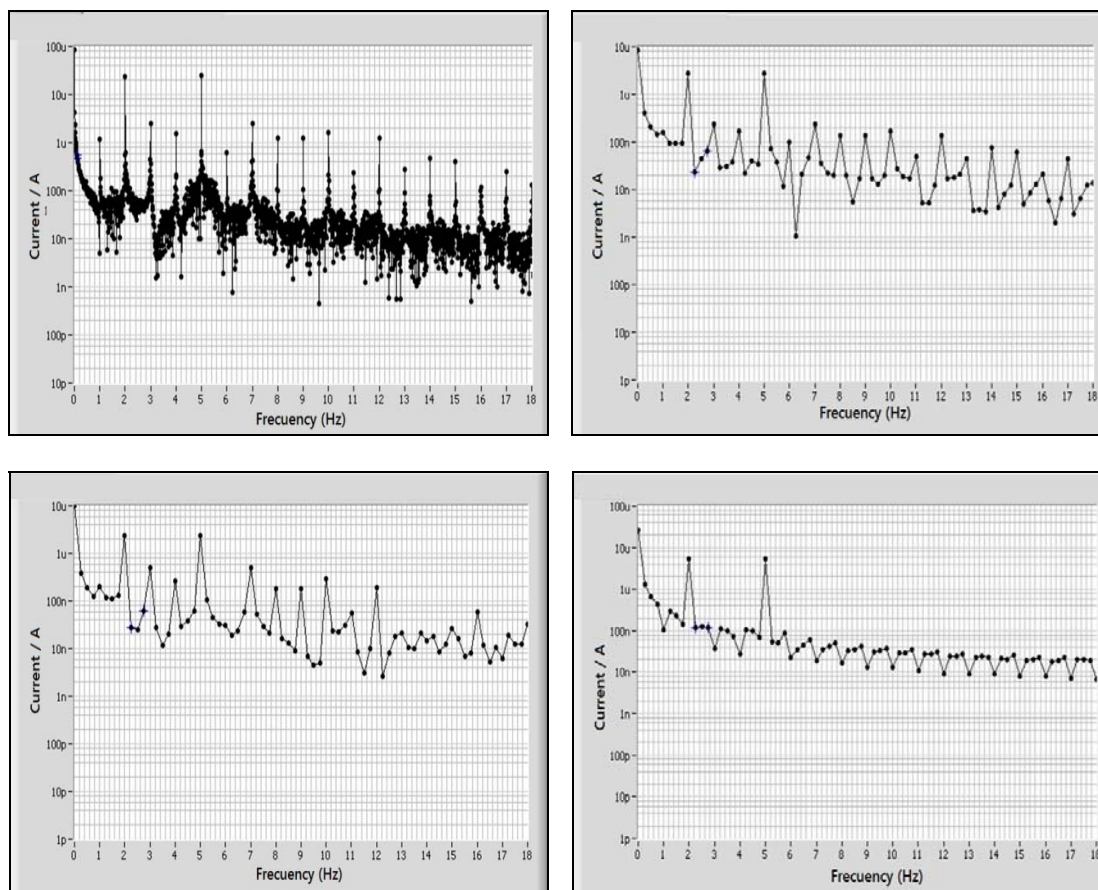


Fig. 4: EFM spectra found in each of the levels of the samples of the steel slag (a) 0 hrs; (b) 3 months; (c) 6 months; (d) 9 months carbonation

From Table 2, results to corrosion rate values of these materials can be observed, that the material at 0 hrs faster evaluation indicates that the specimen evaluated at 3 months, it shows that the carbonation process is affecting the material, but not entirely since increasing the time the passivating layer is generating furthermore compactly, this prevents the material is carbonate and the process of accelerated degradation of the steel, consequently they are corrosion rate values I found below 0 hours, because of that at 0 hours, the formation of this passivation layer is just starting. It is determined that the corrosion potential has decreased; however are not far from each other values, the behavior is appropriate because it indicates that the steel is being protected in this environment, another parameter that varies is minimally the corrosion current, generating a better performance against corrosive phenomena and their cathode and anode parameters, increase in low proportions.

Table 2: Parameters supplied with the EFM technique for concrete obtained with the steel blast furnace slag

	E_{corr} (mV vs Cu/CuSO ₄)	I_{corr} (μ A/cm ²)	V_{corr} (mpy)	Causality Factors 2	Causality Factors 3
0 hours	-284	10.22	0.35	2.3	3.2
3 months	-213	9.31	0.25	1.8	2.8
6 months	-384	13.82	0.68	1.7	2.9
9 months	-391	14.62	0.83	1.9	2.7

CONCLUSION

It is determined that the EFM technique, which is appropriate for the study of this type of material, and it is a technique that thanks to the input frequencies (2 Hz and 5 Hz). We can get the results in no longer than 2 mins, and it is also a non-destructive technique that generates the value of the corrosion current without the need to know the parameters before polarization Tafel slopes (cathode and anode), but generated from the current modulation and inter modulation.

The activated slag concrete has better performance compared with fly ash, against corrosive phenomena when subjected to accelerated carbonation environment in an atmosphere of carbon dioxide, this is because an oxidation protective form. Since the reactions occurring at the interface steel - concrete, are more reactive ceramic matrix of the steel slag.

ACKNOWLEDGEMENT

This research was supported by "Vicerrectoría de investigaciones de la Universidad Militar Nueva Granada" under contract ING 1760.

REFERENCES

1. D. W. Law, J. Cairns, S. G. Millard and J. H. Bungey, *NDT and E. Int.*, **37**, 381 (2004).
2. M. Kouřil, P. Novák and M. Bojko, *Cem. Concr. Compos.*, **28**, 220 (2006).
3. M. E. Mitzithra, F. Deby, J. P. Balayssac and J. Salin, *Nucl. Eng. Des.*, **288**, 42 (2015).
4. K. R. Gowers and S. G. Millard, *Corros. Sci.*, **35**, 1593 (1993).
5. Z. T. Chang, B. Cherry and M. Marosszeky, *Corros. Sci.*, **50**, 357 (2008).
6. V. Kolluru, M. Subramaniam and B. Mingdong, *Corros. Sci.*, **52**, 2725 (2010).
7. Z. T. Chang, B. Cherry and M. Marosszeky, *Corros. Sci.*, **50**, 3078 (2008).
8. M. Alfaro, *Alexandria Engg. J.*, **53**, 977 (2014).
9. Z. Wang, Q. Zeng, L. Wang, Y. Yao and K. Li, *Constr. Build. Mater.*, **53**, 40 (2014).
10. J. Sobhani and M. Najimi, *Constr. Build. Mater.*, **47**, 910 (2013).
11. R. G. Duarte, A. S. Castela, R. Neves, L. Freire and M. F. Montemor, *Electrochim. Acta*, **124**, 218 (2014).
12. S. G. Millard, C. D. Davies and J. H. Bungey, *Coastal Eng.*, **14**, 57 (1990).
13. A. S. Castela, B. Sena da Fonseca, R. G. Duarte, R. Neves and M. F. Montemor, *Electrochim. Acta.*, **124**, 52 (2014).
14. R. Rizwan Hussain, A. Alhozaimy, A. A. Negheimish and D. D. N Singh, *Constr. Build. Mater.*, **73**, 283 (2014).
15. A. Rauf and W. F. Bogaerts, *Corros. Sci.*, **52**, 2773 (2010).
16. A. Rauf and W. F. Bogaerts, *Electrochim. Acta*, **54**, 7357 (2009).
17. L. Han and S. Song, *Corros. Sci.*, **50**, 1551 (2008).
18. S. S. Abdel-Rehim, K. F. Khaled and N. S. Abd-Elshafi, *Electrochim. Acta*, **51**, 3269 (2006).

19. K. F. Khaled, *Mater. Chem. Phys.*, **112**, 290 (2008).
20. L. J. Gardner, S. A. Bernal, S. A. Walling, C. L. Corkhill, John L. Provis and N. C. Hyatt, *Cem. Concr. Res.*, **74**, 78 (2015).
21. N. Marjanović, M. Komljenović, Z. Bašćarević, V. Nikolić and R. Petrović, *Ceram. Int.*, **41**, 1421 (2015).
22. A. Schöler, B. Lothenbach, F. Winnefeld and M. Zajac, *Cem. Concr. Compos.*, **55**, 374 (2015).
23. H. Xu, W. Gong, L. Syltebo, K. Izzo, W. Lutze and I. L. Pegg, *Fuel*, **133**, 332 (2014).
24. P. S. Deb, P. Nath and P. K. Sarker, *Mater. Des.*, **62**, 32 (2014).
25. H. Zhao, W. Sun, X. Wu and Bo Gao, *J. Cleaner Prod.*, **95**, 66 (2015).
26. F. H. Chung, *Environ. Sci. Technol.*, **16**, 796 (1982).
27. N. J. Elton, P. D. Salt, J. M Adams, *Powder Diffr.*, **7**, 71 (1992).
28. S. B. Hassan and V. S. Aigbodion, *Egyptian J. Basic Appl. Sci.*, **1**, 107 (2014).
29. C. Duée, C. Bourgela, E. Véron, M. Allix, F. Fayon, F. Bodéan and J. Poirier, *Cem. Concr. Res.*, **73**, 207 (2015).
30. B. Touzoa, L. K. Scrivenerb and P. Frederic, *Cem. Concr. Res.*, **54**, 77 (2013).
31. A. F. Gualtieria, C. Cavenatib, I. Zanattob, M. Melonib, G. Elmic and M. Lassinantti Gualtieri, *J. Hazard. Mater.*, **152**, 563 (2008).
32. M. N. Piataka, M. B. Parsonsb and R. R. Seal II, *Appl. Geochem.*, **57**, 236 (2015).
33. G. Qiao, Y. Hong, G. Song, H. Li and J. Ou, *Sens. Actuators, B*, **168**, 172 (2012).
34. G. Qiao, Y. Hong and J. Ou, *Meas.*, **67**, 78 (2015).
35. M. J. Correia, E. V. Pereira, M. M. Salta and I. T. E. Fonseca, *Cem. Concr. Compos.*, **28**, 226 (2006).

Accepted : 15.07.2015